PC4230 Computational Project

Manu Magal (A0233509H)

November 25, 2023

Abstract

Using MATLAB, the behaviour of a particle in a harmonic potential subjected to an external perturbation that varies over time was simulated. Numerical analysis determined transition probabilities between eigenstates of the unperturbed system, and these were compared with first-order corrections derived from theory. Analysing the frequency spectra of simulated transitions and observing the correlation between results and the external field's amplitude (A) revealed the dominant order of corrections to transition probabilities. Considering the odd parity of the external field's spatial function, we theoretically predicted and confirmed through simulation that transitions between even eigenstates had zero probability. Acknowledging the limitations in exploring adiabaticity, we suggest further investigation involving time-independent perturbations, specifically employing Wick rotations to approximate the ground state of a perturbed Hamiltonian.

1 Introduction

The study of particle dynamics within harmonic potentials is foundational, providing insights into the fundamental principles governing microscopic systems. The harmonic potential serves as a model for a wide array of phenomena, from molecular vibrations to the behaviour of trapped ions.

One area of interest regarding the harmonic potential is stimulated excitation and de-excitation. This concerns the application of an external potential to the system to coerce the particle to jump between the energy levels of the harmonic potential. This project focuses on a perturbation that varies sinusoidally in time and space. This external potential has various applications in quantum optics, as it represents an electromagnetic standing wave within the particle trap.

In Section 2, the process of simulating the dynamics of the particle using MATLAB is detailed. In Section 3, we present the results of transition probabilities between eigenstates within the simulation (as well as further analysis). In Section 4, limitations of this simulation as well as areas for further investigation are discussed.

2 The Setup

The Hamiltonian of the system is given by

$$\hat{H} = \frac{\hat{p}^2}{2} + \frac{1}{2}x^2 + A\sin(x)\cos(\omega t) \tag{1}$$

where the term in blue is the external field. A is the amplitude of the external field and ω is its driving fequency.

The simulation aspect of the project relies on approximating the position and momentum of the particle (which are continuous in reality) as well as time as discrete variables. It is assumed that the step-lengths chosen are small enough that minimal information is lost, and the overall fidelity of the simulation is retained. This is verified by checking the fundamental results of the simulation (such as time-evolution of a

harmonic eigenstate) for convergence. Upon doing so, we choose step-lengths which maintain the fidelity of the simulation, but also remain computationally feasible to execute.

Another crucial aspect of simulation is evolving the state of the particle in order to simulate quantum dynamics. The Split-Operator (SO) method is used to do so. The steps for the SO method are as follows:

1. Apply $e^{-iV\frac{\Delta t}{2}}$ at time t to the state at time t. Since the state is in the position representation by default, $e^{-iV\frac{\Delta t}{2}}$ is a diagonal matrix, making calculations efficient.
2. Use the `fft` function in MATLAB to convert the state from the position representation to the momentum representation.
3. Apply $e^{-iT\Delta t}$ at time t to the state. Since the state is now in the momentum representation, $e^{-iT\Delta t}$ can be represented with a diagonal matrix, making calculations efficient.
4. Use the `ifft` function in MATLAB to revert the state from the momentum representation to the position representation.
5. Apply $e^{-iV\frac{\Delta t}{2}}$ at time t to the state. This final output is the state in position representation at time $t + \Delta t$.

We note that the SO method is an approximation of the time evolution of the state, but our efforts to verify convergence ensure that the approximation is reliable.

The parameters of the simulation are as follows:

- Width of Simulation, L: 40
- Location of Wavepacket, x_0: 0
- Width of Initial Wavepacket, σ: 1

Varying x_0 and σ will result in different results for most of the investigation conducted in this report. $x_0 = 0$ was chosen as it is the most likely location of the wavepacket in the harmonic trap before a perturbation is applied. $\sigma = 1$ was chosen as it simplifies calculations significantly. In general, the results of this report can be viewed as a baseline against which more exotic values of x_0 and σ can be compared.

The duration of the simulation, T, is a parameter that is varied for different experiments to view processes which occur over larger time scales. The time step is adjusted accordingly for any variation in T to ensure convergence of results.

3 Transition Probability Analysis

The main topic of interest in the analysis of this potential is the transition probability between eigenstates of the harmonic potential when the driving frequency of the perturbation is on-resonance with the natural frequency of the harmonic potential (which is 1, in the dimensionless case). We investigate 4 scenarios:

1. The transition probability from the ground state $|\psi_0\rangle$ to the first excited state $|\psi_1\rangle$ when $\omega \approx 1.0$.
2. The 2-photon transition probability from the ground state $|\psi_0\rangle$ to the first excited state $|\psi_1\rangle$ when $\omega \approx 0.5$.
3. The transition probability from the ground state $|\psi_0\rangle$ to the second excited state $|\psi_2\rangle$ when $\omega \approx 2.0$.
4. The transition probability from the ground state $|\psi_0\rangle$ to the fourth excited state $|\psi_4\rangle$ when $\omega \approx 2.0$.

From Born's Rule, we know that the probability of transition between 2 states is given by

$$P = |\langle\phi|\psi\rangle|^2 \tag{2}$$

This quantity can be measured within the simulation by taking the inner product of the state of the particle, $|\psi(t)\rangle$, with the desired state, $|\phi\rangle$, at every time step.

Additionally, from our lectures, we know that the first-order correction to the transition probability between 2 states is given by

$$P_{n\leftarrow m} = \left| \int_0^t dt_1 \, \langle\psi_n| \, \hat{V}(t_1) \, |\psi_m\rangle \, e^{i(E_n - E_m)t_1} \right|^2 \tag{3}$$

and the second-order correction to the transition probability between 2 states is given by

$$P_{n\leftarrow m} = \left| \int_0^t dt_1 \int_0^{t_1} dt_2 \, \langle\psi_n| \, \hat{U_0}^\dagger(t_1, 0)\hat{V}(t_1)\hat{U_0}(t_1, 0)\hat{U_0}^\dagger(t_2, 0)\hat{V}(t_2)\hat{U_0}(t_2, 0) \, |\psi_m\rangle \right|^2 \tag{4}$$

Development of Eq. 4 to obtain a more general form is presented in Annex A. Throughout this section, we will utilise Eq. 3 and the simulation of Eq. 2 to investigate the transition probabilities.

The 2 parameters which are of importance in this section are A and ω. The perturbative theory requires that A is small, so we expect the simulation to break down for larger values of A. The on-resonance condition asserts that ω is close to ω_{mn}, the transition frequency between the 2 states. Thus, it is expected that the smaller the difference in ω and ω_{mn}, the greater the transition probability. These initial hunches will be investigated through the following analysis.

3.1 $|\psi_0\rangle \rightarrow |\psi_1\rangle$, $\omega \approx 1.0$

We first run the simulation for different values of ω, keeping A constant at 0.01.

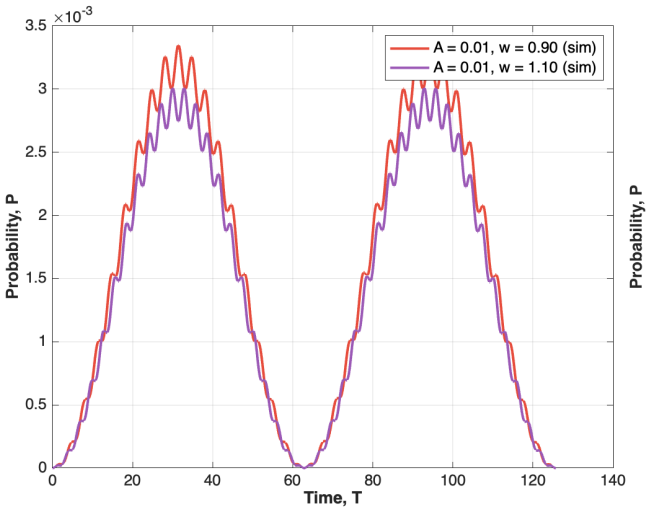

Figure 1: *Plot of P against T for $|\psi_0\rangle \rightarrow |\psi_1\rangle$. $\omega = 0.90/1.10,\ A = 0.01.$*

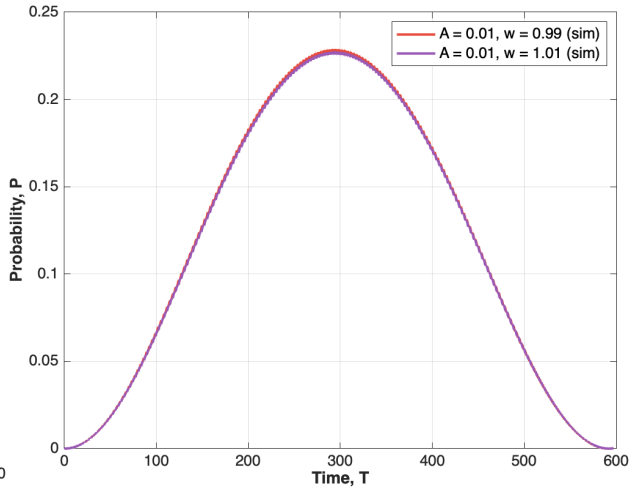

Figure 3: *Plot of P against T for $|\psi_0\rangle \rightarrow |\psi_1\rangle$. $\omega = 0.99/1.01,\ A = 0.01.$*

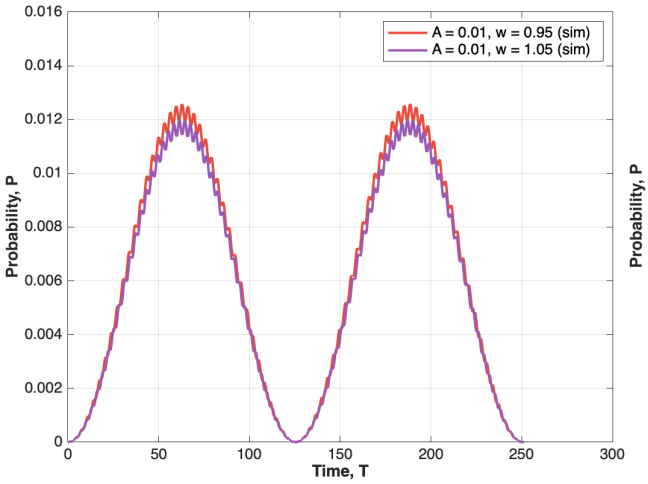

Figure 2: *Plot of P against T for $|\psi_0\rangle \rightarrow |\psi_1\rangle$. $\omega = 0.95/1.05,\ A = 0.01.$*

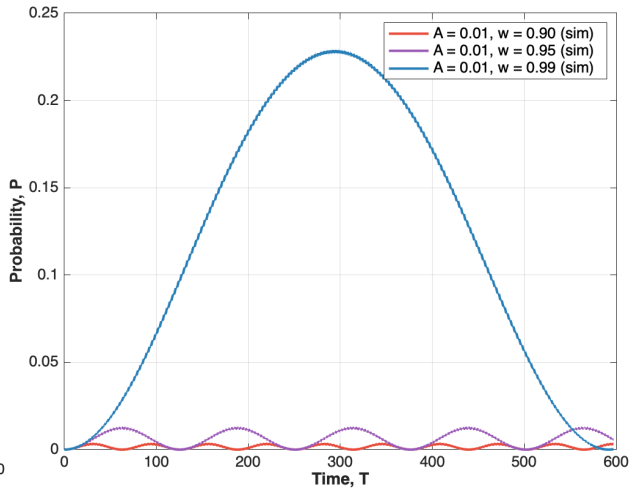

Figure 4: *Plot of P against T for $|\psi_0\rangle \rightarrow |\psi_1\rangle$. $\omega = 0.90, 0.95/0.99,\ A = 0.01.$*

A few observations can be made from the figures above. Firstly, P oscillates with different frequencies (one may suggest that the smaller the value of $|\omega - 1|$, the smaller the frequency of oscillations of P). Secondly, the smaller the value of $|\omega - 1|$, the larger the amplitude of P. This makes sense as the a smaller value of $|\omega - 1|$ indicates that the driving frequency is more on-resonance with the harmonic potential, thus causing the likelihood of transition to be greater.

Thirdly, for any 2 graphs with the same value of $|\omega - 1|$, the graph with $\omega < 1$ has larger values of P than the graph with $\omega > 1$. Lastly, taking a closer look at Figures 1 through 3, 2 oscillations can be observed: a relatively slower oscillation with large amplitude, and a much faster oscillation with small amplitude. The explanations for these 2 phenomena will be left for later.

Next, we derive the transition probability suggested by theory. Utilising Eq. 3 and substituting $m = 0$ and $n = 1$,

$$\begin{aligned}
&\int_0^t dt_1 \, \langle \psi_1 | \, \hat{V}(t_1) \, | \psi_0 \rangle \, e^{i(E_1 - E_0)t_1} \\
&= A\sqrt{\frac{2}{\pi}} \int_0^t dt_1 \cos(\omega t_1) e^{it_1} \int_{-\infty}^{\infty} dx \; x e^{-x^2/2} \sin(x) e^{-x^2/2} \\
&= A\sqrt{\frac{2}{\pi}} \int_0^t dt_1 \, \frac{1}{2} \left(e^{i\omega t_1} + e^{-i\omega t_1} \right) e^{it_1} \left(\frac{e^{-1/4}}{8} \right) \left[\sqrt{\pi} \left(\text{erf}\left(x + \frac{i}{2} \right) + \text{erf}\left(x - \frac{i}{2} \right) \right) - 4e^{1/4} e^{-x^2} \sin(x) \right]_{-\infty}^{\infty} \\
&= A \left(\frac{\sqrt{2}}{2} \right) \left(\frac{e^{i(1-\omega)t} - 1}{i(1-\omega)} \right) \left(e^{-1/4} \right) \left(\frac{4}{8} \right) \; (E_2 > E_1 \text{ so second term in time integral dominates}) \\
&= \frac{A}{4} \sqrt{2} e^{-1/4} \frac{e^{i(1-\omega)t} - 1}{i(1-\omega)}
\end{aligned}$$

Note that the Rotating Wave Approximation was invoked to drop the non-dominant term in the time integal. Thus, the probability of transition from the ground state to the first excited state is

$$P_{1 \leftarrow 0} = \frac{A^2}{8} e^{-1/2} \left| \frac{e^{i(1-\omega)t} - 1}{1 - \omega} \right|^2 \tag{5}$$

The theoretical probabilities are plotted with the simulated probabilities for $\omega = 0.95$ and $\omega = 0.99$, with 3 different values of A.

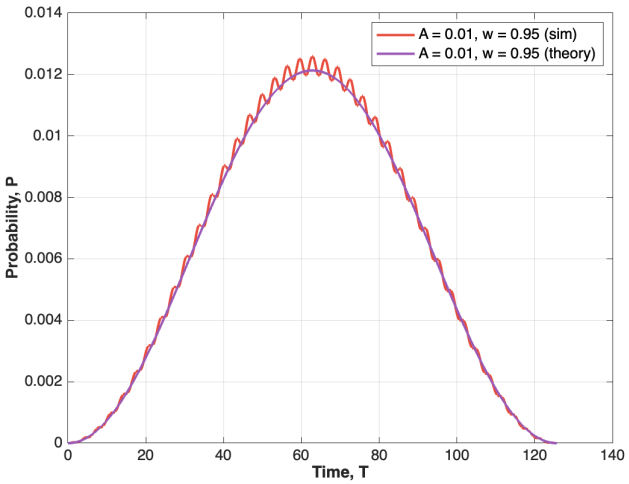

Figure 5: *Plot of P against T for $|\psi_0\rangle \rightarrow |\psi_1\rangle$. $\omega = 0.95$, $A = 0.01$.*

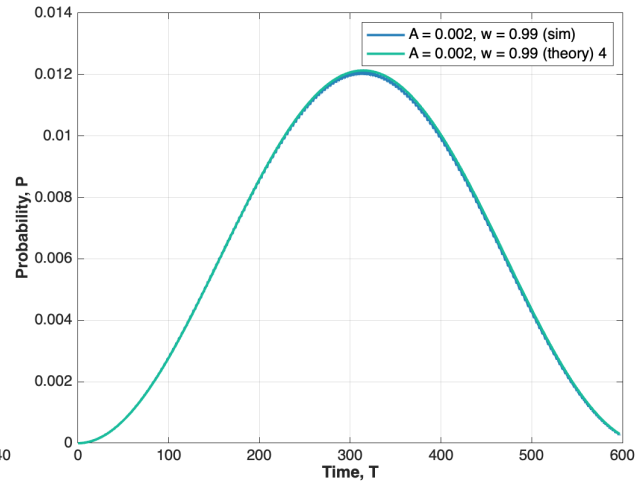

Figure 6: *Plot of P against T for $|\psi_0\rangle \rightarrow |\psi_1\rangle$. $\omega = 0.99$, $A = 0.002$.*

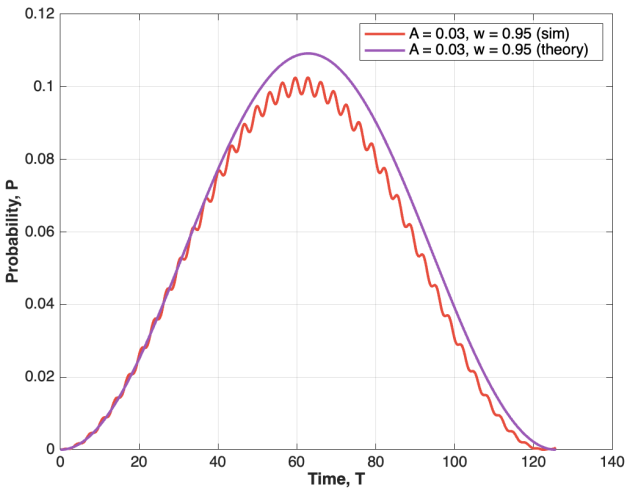

Figure 7: *Plot of P against T for $|\psi_0\rangle \to |\psi_1\rangle$. $\omega = 0.95,\ A = 0.03$.*

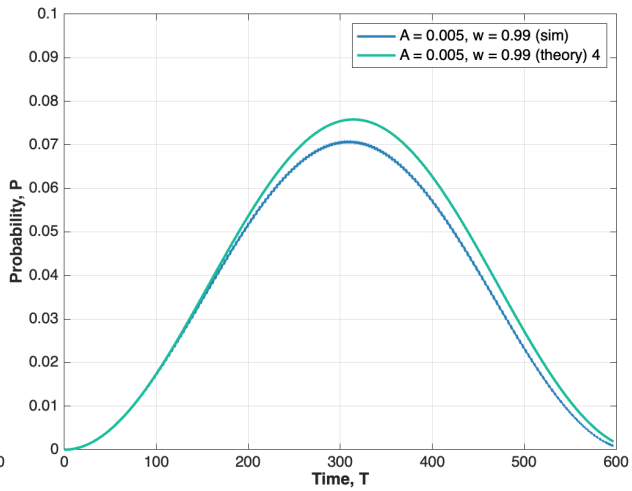

Figure 9: *Plot of P against T for $|\psi_0\rangle \to |\psi_1\rangle$. $\omega = 0.99,\ A = 0.005$.*

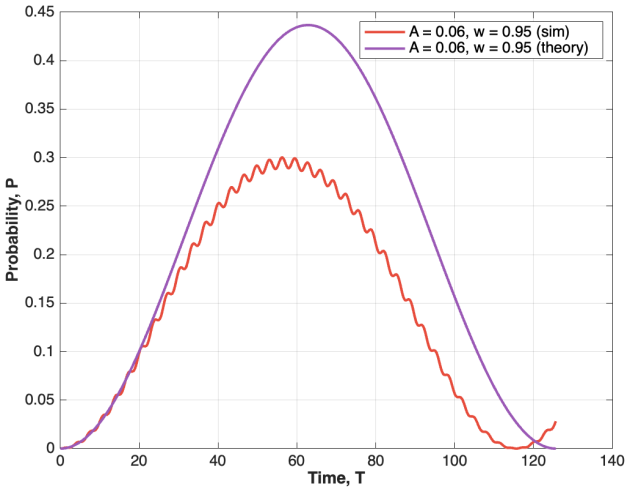

Figure 8: *Plot of P against T for $|\psi_0\rangle \to |\psi_1\rangle$. $\omega = 0.95,\ A = 0.06$.*

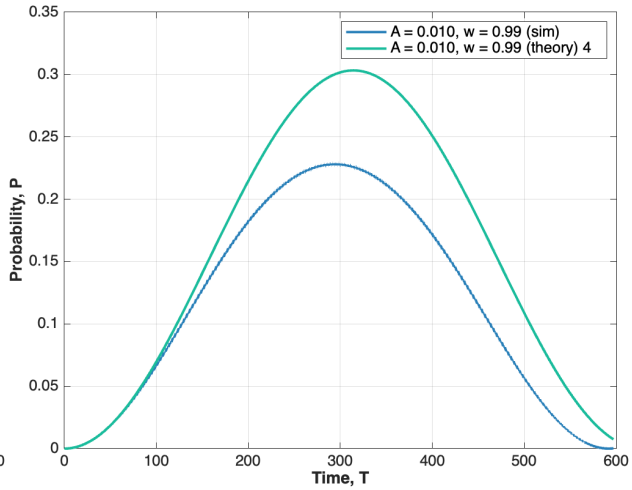

Figure 10: *Plot of P against T for $|\psi_0\rangle \to |\psi_1\rangle$. $\omega = 0.99,\ A = 0.01$.*

We see from Figures 5 and 6 that the plots of Eq. 5 corresponding to each graph fits very well for small values of A. Eq. 5 indicates that the smaller the value of $|\omega - 1|$, the smaller the frequency of the oscillatory term in $P_{1\leftarrow 0}$, and the smaller the frequency of oscillations of P. Additionally, the dropping of the non-dominant term in the RWA explains the lack of weak high-frequency oscillations in the plots of the theoretical transition probabilities. The low-frequency oscillations mentioned earlier are accounted for by the dominant term in $P_{1\leftarrow 0}$, and the high-frequency oscillations are accounted for by the non-dominant term.

However, Figures 7 through 10 show a deviation between the simulated and theoretical plots, which increases as A increases. Eq. 5 indicates that A^2 and $\frac{1}{|1-\omega|}$ both serve to increase $P_{1\leftarrow 0}$ (as A increases and ω becomes closer to 1). $P_{1\leftarrow 0}$ clearly has to be less than 1, which constrains the magnitudes of A^2 and $\frac{1}{|1-\omega|}$. Thus, Eq. 5 starts to fail as is it increases, thereby explaining the discrepancy between the simulated and theoretical transition probabilities. Naturally, more stock should be put in the simulated transition probabilities as a model for reality as they are simulated measurements of the system.

3.2 $|\psi_0\rangle \rightarrow |\psi_1\rangle$, $\omega \approx 0.5$

If ω were to be approximately equal to 0.5, it is expected that one-photon transitions are less likely, and two-photon transitions are more probable.

Since ω is off-resonance, there is no non-dominant term to discard from $P_{1\leftarrow 0}$, as both terms will provide significant contributions. Thus,

$$P_{1\leftarrow 0} = \frac{A^2}{8} e^{-1/2} \left| \frac{e^{i(1-\omega)t} - 1}{1-\omega} + \frac{e^{i(1-\omega)t} - 1}{1-\omega} \right|^2 \tag{6}$$

To examine this transition, the simulation is run for different values of A, keeping ω constant at $\omega = 0.45$ and $\omega = 0.49$. The first-order theoretical transition probabilities are also plotted to be compared against.

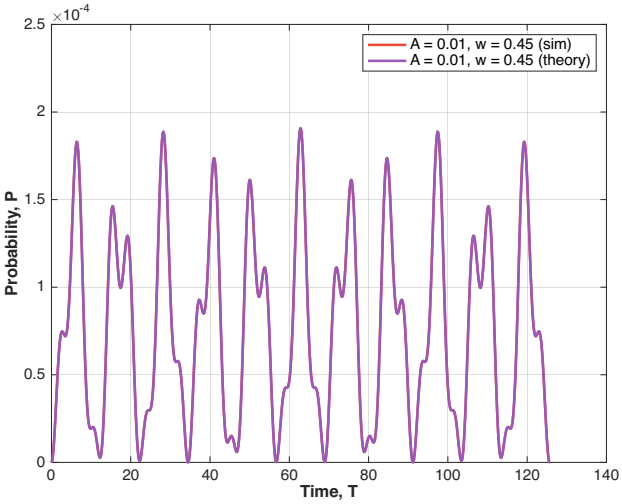

Figure 11: *Plot of P against T for $|\psi_0\rangle \rightarrow |\psi_1\rangle$. $\omega = 0.45,\ A = 0.01$.*

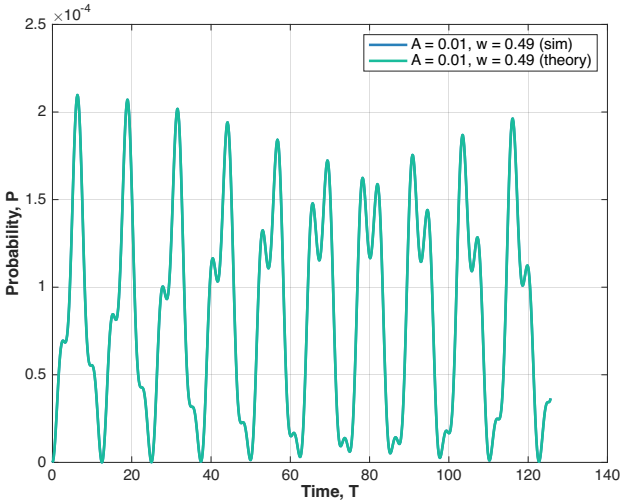

Figure 13: *Plot of P against T for $|\psi_0\rangle \rightarrow |\psi_1\rangle$. $\omega = 0.49,\ A = 0.01$.*

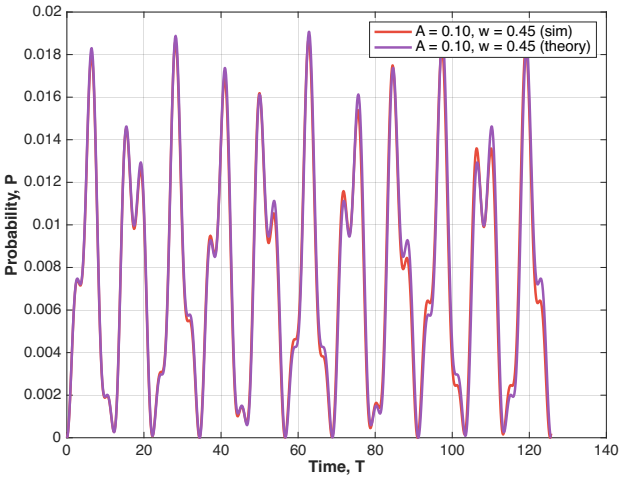

Figure 12: *Plot of P against T for $|\psi_0\rangle \rightarrow |\psi_1\rangle$. $\omega = 0.45,\ A = 0.1$.*

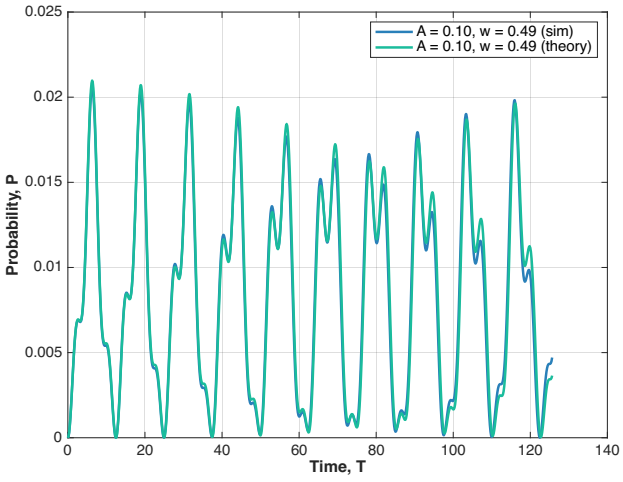

Figure 14: *Plot of P against T for $|\psi_0\rangle \rightarrow |\psi_1\rangle$. $\omega = 0.49,\ A = 0.1$.*

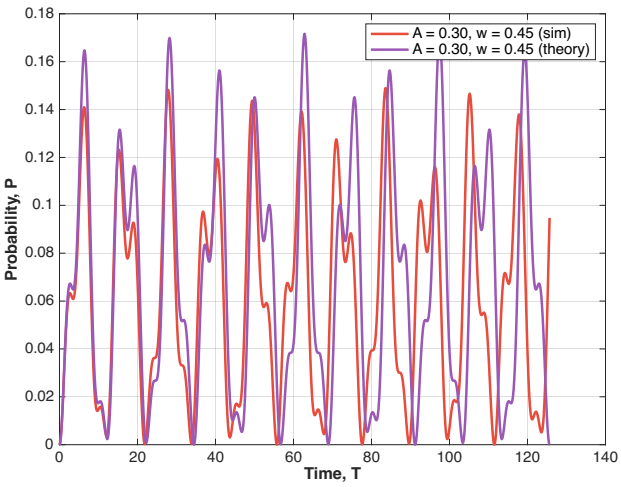

Figure 15: *Plot of P against T for $|\psi_0\rangle \to |\psi_1\rangle$. $\omega = 0.45,\ A = 0.3$.*

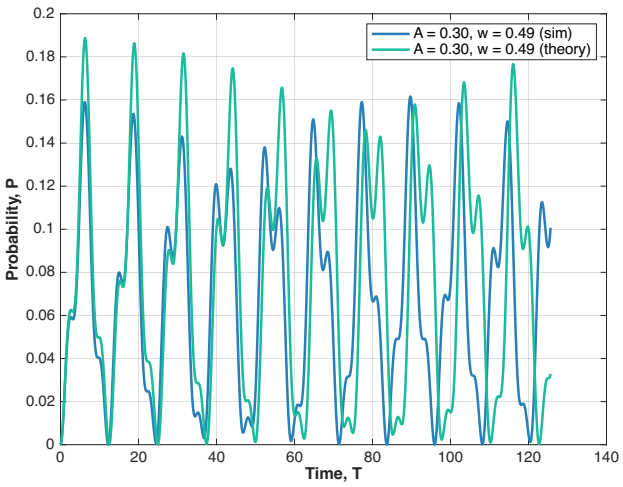

Figure 16: *Plot of P against T for $|\psi_0\rangle \to |\psi_1\rangle$. $\omega = 0.49,\ A = 0.3$.*

Figures 11 through 14 indicate very little deviation between simulated transition probability and the theoretical first-order transition probability. It is only when A becomes significantly large (Figures 15 & 16) that we see deviation between the simulated and theoretical transition probabilities (although this may also be due to the aforementioned effect of the theoretical formula failing at higher values of A).

These observations give credence to the possibility that the 2-photon transition process $|\psi_0\rangle$ to $|\psi_1\rangle$ has a very low probability of occurring, which is opposite to our initial hypothesis.

3.3 $|\psi_0\rangle \to |\psi_2\rangle$, $\omega \approx 2$

We begin this subsection by deriving the theoretical transition probability. Utilising Eq. 3 and substituting $m = 0$ and $n = 2$,

$$\int_0^t dt_1 \langle\psi_2| \hat{V}(t_1) |\psi_0\rangle e^{i(E_2 - E_0)t_1} = A\sqrt{\frac{1}{2\pi}} \int_0^t dt_1 \cos(\omega t_1) e^{i2t_1} \int_{-\infty}^{\infty} dx \underbrace{\left(2x^2 - 1\right) e^{-x^2/2} \sin(x) e^{-x^2/2}}_{\text{integrand is odd}} = 0$$

We are able to conclude that the expression is identically equal to 0 as the integrand in the spatial integral is odd. In general, due to the fact that the even eigenstates of the harmonic potential have even parity and the perturbation has odd parity, all one-photon transitions between even eigenstates will be 0.

This is verified using the simulation, which is run for $\omega = 1.95$ and $\omega = 1.99$, with different values of A.

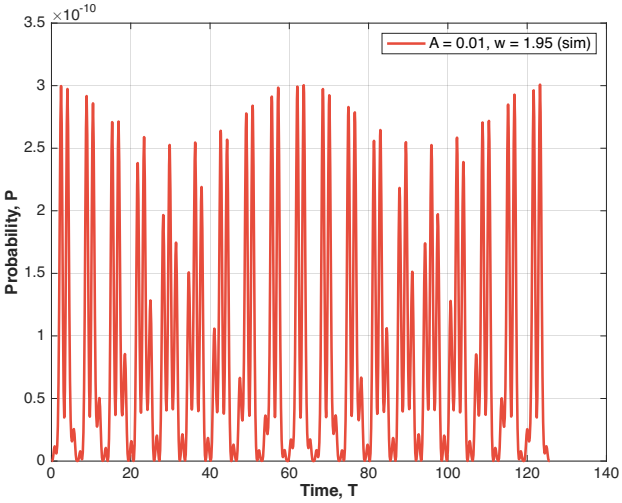

Figure 17: *Plot of P against T for $|\psi_0\rangle \to |\psi_2\rangle$. $\omega = 1.95,\ A = 0.01$.*

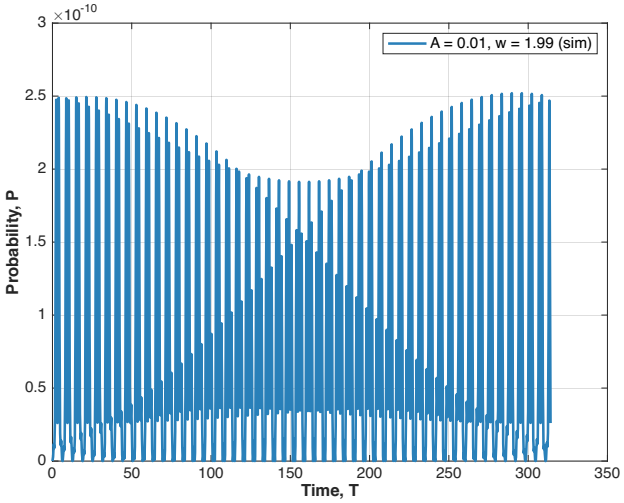

Figure 19: *Plot of P against T for $|\psi_0\rangle \to |\psi_2\rangle$. $\omega = 1.99,\ A = 0.01$.*

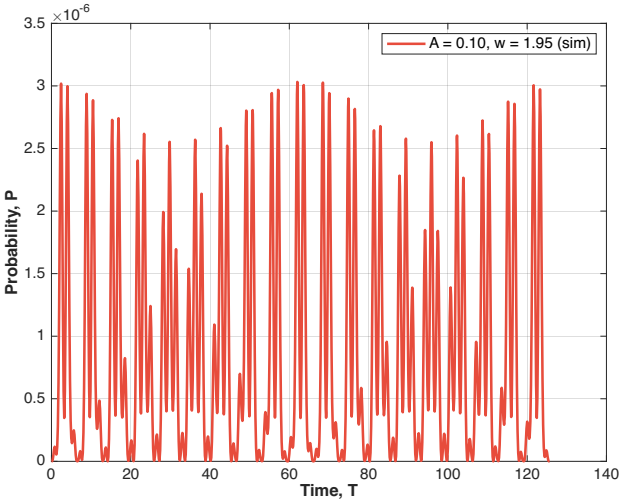

Figure 18: *Plot of P against T for $|\psi_0\rangle \to |\psi_2\rangle$. $\omega = 1.95,\ A = 0.1$.*

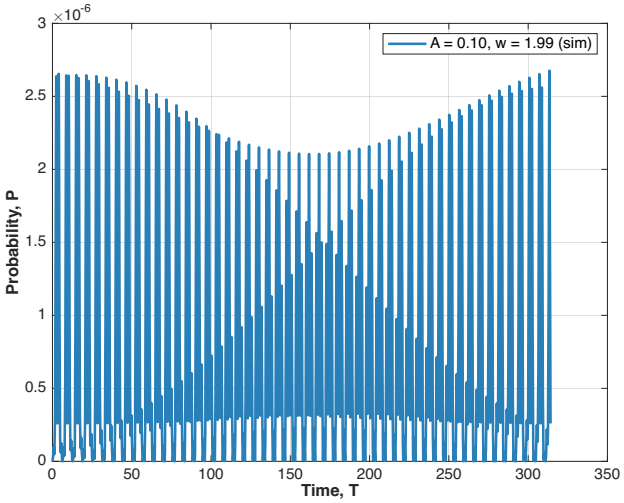

Figure 20: *Plot of P against T for $|\psi_0\rangle \to |\psi_2\rangle$. $\omega = 1.99,\ A = 0.1$.*

Figures 17 through 20 give an indication that one-photon transitions are not occurring, due to the very small amplitudes of P. The graphs have multiple modes of oscillation. Additionally, since P increased by a factor of 10^4 upon the incease of A by a factor of 10 for both values of A, we can deduce that the simulated transition probabilities are likely not random noise. A Fourier transform of all 4 graphs is conducted to investigate their frequency spectra.

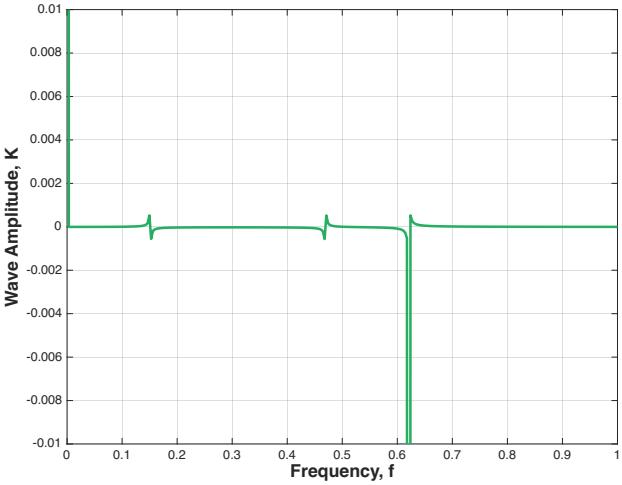

Figure 21: *Plot of K against f for* $|\psi_0\rangle \to |\psi_2\rangle$. $\omega = 1.95,\ A = 0.01$. *Peaks occur at* $f = 0.0032, 0.15, 0.47, 0.62$.

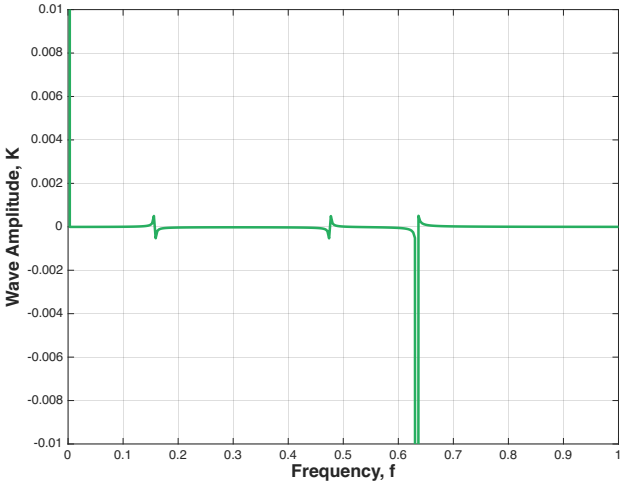

Figure 23: *Plot of K against f for* $|\psi_0\rangle \to |\psi_2\rangle$. $\omega = 1.99,\ A = 0.01$. *Peaks occur at* $f = 0.0032, 0.155, 0.475, 0.635$.

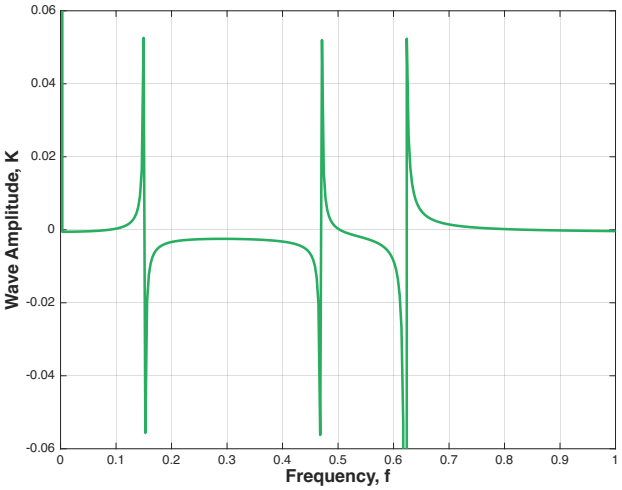

Figure 22: *Plot of K against f for* $|\psi_0\rangle \to |\psi_2\rangle$. $\omega = 1.95,\ A = 0.1$. *Peaks occur at* $f = 0.0032, 0.15, 0.47, 0.62$.

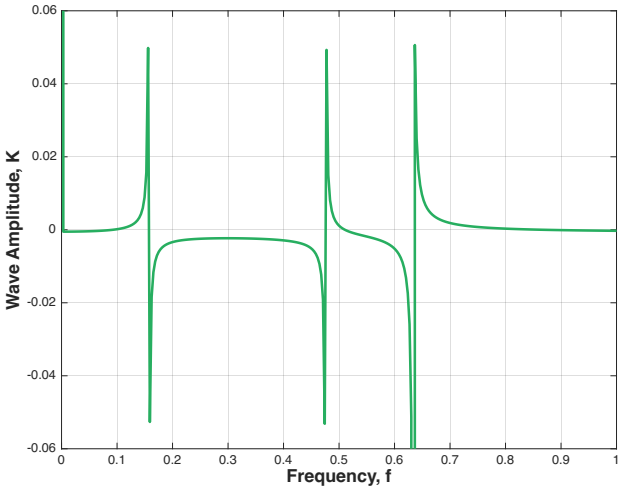

Figure 24: *Plot of K against f for* $|\psi_0\rangle \to |\psi_2\rangle$. $\omega = 1.99,\ A = 0.1$. *Peaks occur at* $f = 0.0032, 0.155, 0.475, 0.635$.

Figures 21 through 24 indicate that there are unusual peaks at $f \approx 0.15$ and $f \approx 0.47$, which also increase in response to an increase in A. From Eq. 4, we know that the second-order correction to the transition probability is directly proportional to A^4, so an increase in A by a factor of 10 would cause an increase in P by a factor of 10^4. With this knowledge as well as our observations from Figures 17 through 20, we conclude that the observed transition probabilities are due to two-photon processes.

3.4 $|\psi_0\rangle \to |\psi_4\rangle$, $\omega \approx 2$

As mentioned earlier, any one-photon transition between 2 even eigenstates will have 0 probability of occurring (at least according to theory). However, since $\omega \approx 2$, we expect 2-photon transitions from $|\psi_0\rangle$ to $|\psi_4\rangle$ to be likely.

To test this, the simulation is run for $\omega = 1.95$ and $\omega = 1.99$, with different values of A.

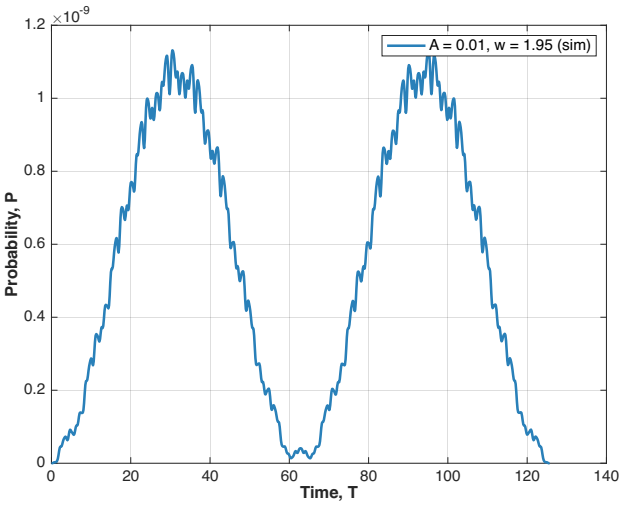

Figure 25: $\omega = 1.95$, $A = 0.01$

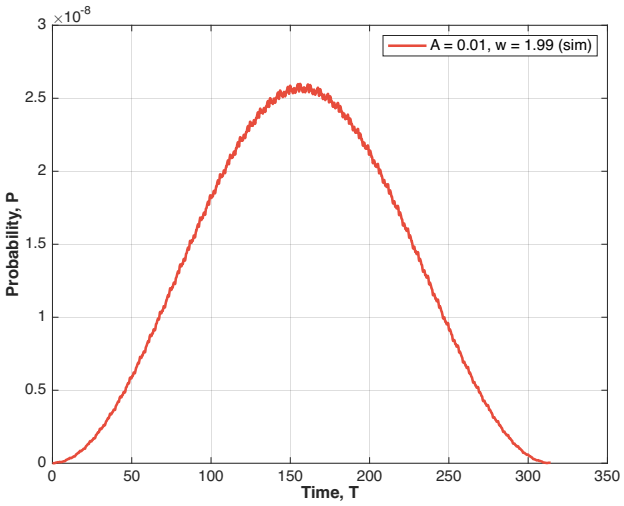

Figure 27: $\omega = 1.99$, $A = 0.01$

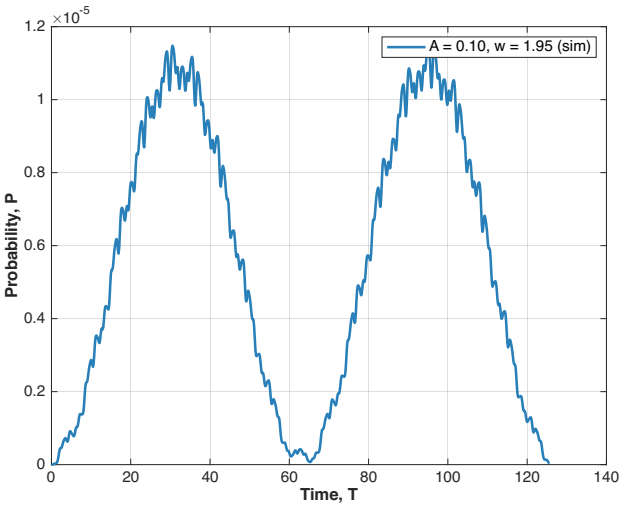

Figure 26: $\omega = 1.95$, $A = 0.1$

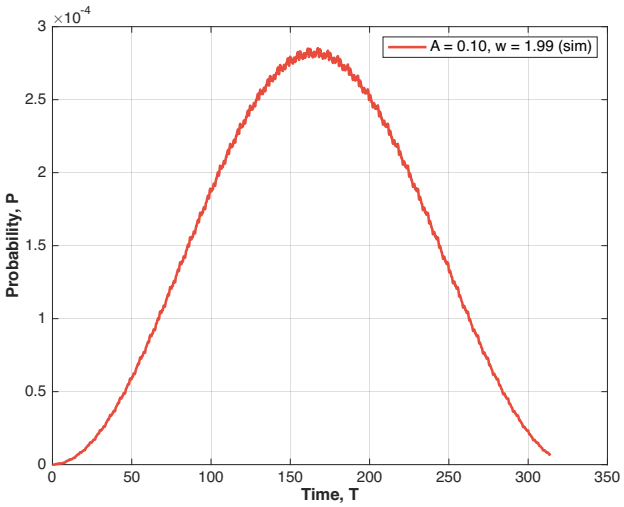

Figure 28: $\omega = 1.99$, $A = 0.1$

We also investigate the frequency spectra of the graphs (Figures 29 through 32). These figures tell us much of the same information as the frequency spectra in the previous subsection – that there are unusual peaks at $f \approx 0.15$ and $f \approx 0.47$ whose wave amplitudes increase with increasing A. Furthermore, we can observe from Figures 25 through 28 that an increase in A by a factor of 10 corresponds to an increase in P by a factor of 10^4. Thus, we can conclude that the observed transition probabilities are mainly caused by 2-photon processes.

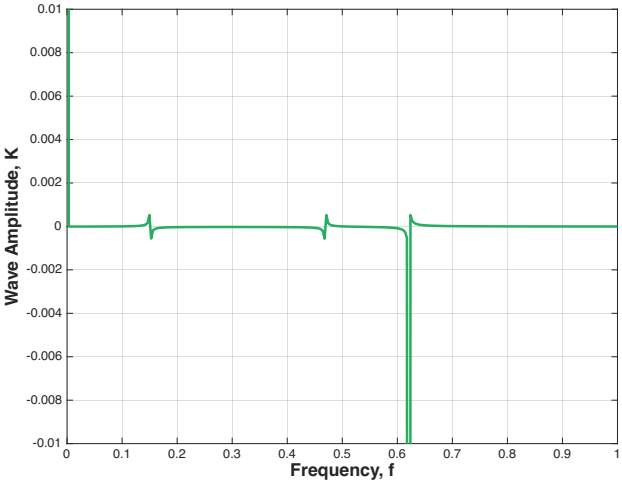

Figure 29: *Plot of K against f for $|\psi_0\rangle \to |\psi_4\rangle$. $\omega = 1.95,\ A = 0.01$. Peaks occur at $f = 0.0032, 0.15, 0.47, 0.62$.*

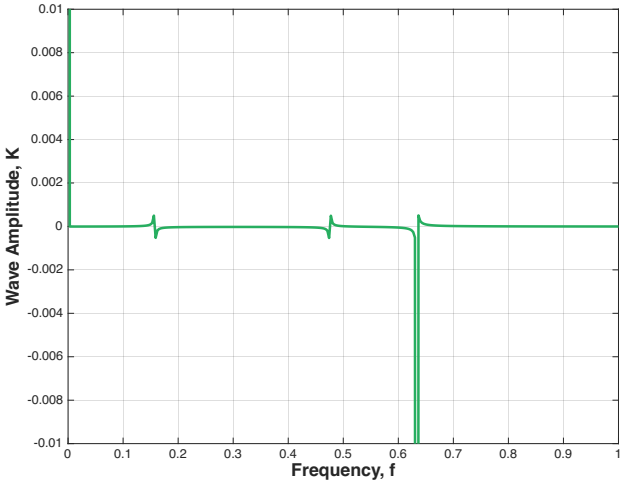

Figure 31: *Plot of K against f for $|\psi_0\rangle \to |\psi_4\rangle$. $\omega = 1.99,\ A = 0.01$. Peaks occur at $f = 0.0032, 0.157, 0.476, 0.633$.*

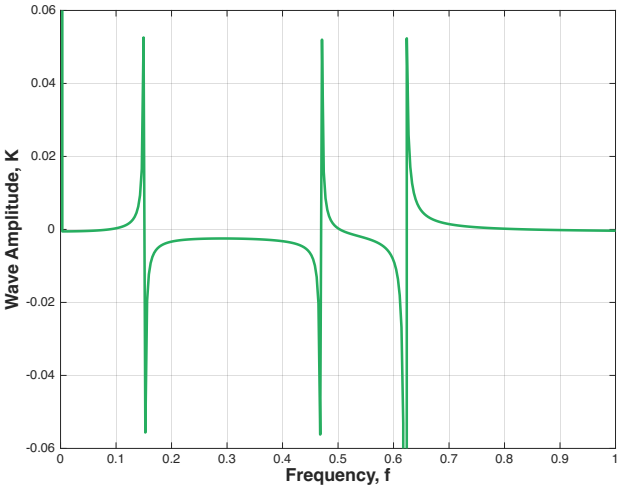

Figure 30: *Plot of K against f for $|\psi_0\rangle \to |\psi_4\rangle$. $\omega = 1.95,\ A = 0.1$. Peaks occur at $f = 0.0032, 0.15, 0.47, 0.62$.*

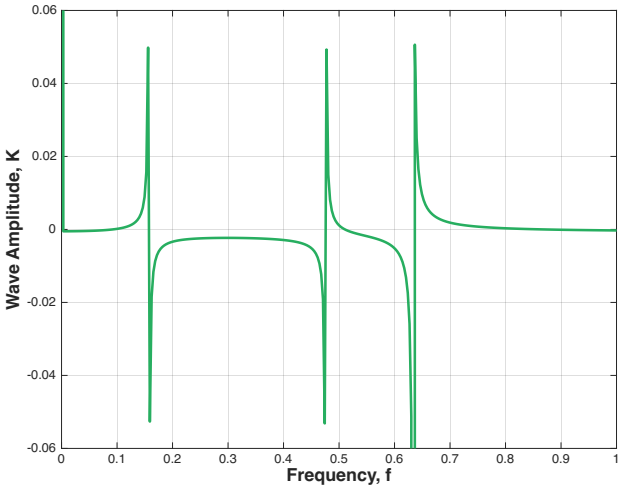

Figure 32: *Plot of K against f for $|\psi_0\rangle \to |\psi_4\rangle$. $\omega = 1.99,\ A = 0.1$. Peaks occur at $f = 0.0032, 0.157, 0.476, 0.633$.*

4 Limitations & Further Investigations

Although we achieved all the results we sought to attain, we were unable to perform certain experiments to determine further results. One such experiment was to simulate adiabatic time evolution of the system to determine the variation in the energy levels of the system over time.

As we learned from the lectures, when a system evolves adiabatically, an eigenstate of the original unperturbed Hamiltonian will remain as an eigenstate of the evolving Hamiltonian for all time. Our intention was to define the initial state $|\psi\rangle$ as an eigenstate of the harmonic potential, then evolve both $|\psi\rangle$ and $\hat{H}$ over time, calculating $\langle\psi|\hat{H}|\psi\rangle$ at each time step.

However, if ω was increased to the point that the system evolves diabatically, then $\langle\psi|\hat{H}|\psi\rangle$ would just give the expectation value of the energy of the particle when measured, with no way of determining if $|\psi\rangle$ is still an eigenstate of the Hamiltonian at time t. Thus, this methodology was abandoned, and other methods will have to be found to verify that $|\psi\rangle$ remains an eigenstate of the system for all time.

Another potential area for investigation involves the usage of a Wick rotation of time in order to approximate the ground state of a time-independent Hamiltonian. Let us assume the perturbed Hamiltonian of the system was time-independent, like so:

$$H = \frac{p^2}{2} + \frac{x^2}{2} + A\sin(x) \tag{7}$$

An arbitrary state at time t can be expressed as

$$|\Psi(t)\rangle = \sum_i U(t,0)\,|\psi_i\rangle \tag{8}$$

where $|\psi_i\rangle$ are the eigenstates of the unperturbed Hamiltonian (this can be done as the eigenstates of the harmonic oscillator form a complete basis). Now, if we perform the transformation $t \to -it$ and evolve the states, the time evolution operator serves to decay terms with higher energies in the perturbed Hamiltonian. Thus, over time, the states with lower energies will dominate in the sum, causing $|\Psi\rangle$ to evolve to approximate the ground state of the perturbed Hamiltonian. Further details can be found in [1].

5 Conclusion

Through application of various computational techniques, the dynamics of a microscopic particle in a harmonic potential subject to an external time-varying perturbation was simulated. The transition probabilities between different energy levels of the unperturbed system were determined numerically and compared with the first-order corrections to the transition probabilities, which were derived from time-dependent perturbation theory. On-resonance transitions were investigated by tweaking the frequency (ω) of the external field to match the transition frequencies of the energy levels. Through analysis of the frequency spectra of the simulated transition probabilities as well as the increase in order of results with a corresponding increase in amplitude (A) of the external field, the results of the simulation were correlated with the dominant order amongst the corrections to the transition probability. Due to the external field being composed of a spatial function of odd parity, we determined from theory that all transitions between even eigenstates would have 0 probability of occurring, and this was matched by the results of the simulation for $|\psi_0\rangle \to |\psi_2\rangle$ with ω set to approximately 2.

In addition, we noted the limitations of our simulation in exploring adiabaticity, and proposed further investigation of time-independent perturbations in the form of Wick rotations to find an approximate ground state of the perturbed Hamiltonian.

References

[1] Lehtovaara, L., Toivanen, J., & Eloranta, J. (2007). *Solution of time-independent Schrödinger equation by the imaginary time propagation method.* Journal of Computational Physics, 221(1), 148–157. https://doi.org/10.1016/j.jcp.2006.06.006

Annex A: Mathematical Derivations

$|\psi_0\rangle \to |\psi_1\rangle$ First-Order Transition Spatial Integral

$$\begin{aligned}
\int_{-\infty}^{\infty} dx\, x\sin(x)e^{-x^2} &= \frac{i}{2}\int_{-\infty}^{\infty} dx\, x\left(e^{ix}-e^{-ix}\right)e^{-x^2} \\
&= \frac{i}{2}\int_{-\infty}^{\infty} dx\, xe^{ix-x^2} - \frac{i}{2}\int_{-\infty}^{\infty} dx\, xe^{-ix-x^2} \\
&= \frac{i}{2}\int_{-\infty}^{\infty} dx\, xe^{ix-x^2} - \frac{i}{2}\int_{\infty}^{-\infty} -dw\, (-w)e^{iw-w^2} \text{ (Substitute } x=-w) \\
&= \frac{i}{2}\int_{-\infty}^{\infty} dx\, xe^{ix-x^2} + \frac{i}{2}\int_{-\infty}^{-\infty} dw\, we^{iw-w^2} \\
&= i\int_{-\infty}^{\infty} dx\, xe^{ix-x^2} \\
&= i\int_{-\infty}^{\infty} dx\, xe^{-1/4}e^{-(x-i/2)^2}
\end{aligned}$$

This is a complex integral which I do not have the knowledge to solve. However, many texts list out the steps to complete this integral and obtain the desired result. I personally used the website https://www.integral-calculator.com to carry out the integration.

General Second-Order Correction to Transition Probability

We label $|k\rangle$ as the k-th eigenstate of the harmonic oscillator. Let $V(t) = A\cos(\omega t)K$ such that $K_{nm} = \langle n|K|m\rangle = \int_{-\infty}^{\infty} H_n(x)\sin(x)H_m(x)\,dx$ (with appropriate normalisation factors for $|n\rangle$ and $|m\rangle$).

$$\begin{aligned}
&\langle n|\int_0^t dt_1\int_0^{t_1} dt_2\; V_I(t_1)V_I(t_2)\,|m\rangle \\
&= \int_0^t dt_1\int_0^{t_1} dt_2\;\langle n|\,U_0^\dagger(t_1,0)V(t_1)U_0(t_1,0)U_0^\dagger(t_2,0)V(t_2)U_0(t_2,0)\,|m\rangle \\
&= \int_0^t dt_1\int_0^{t_1} dt_2\;\sum_k e^{iE_nt_1}\langle n|\,V(t_1)U_0(t_1,0)\,|k\rangle\,\langle k|\,U_0^\dagger(t_2)V(t_2)\,|m\rangle\,e^{-iE_mt_2} \\
&= A^2\int_0^t dt_1\int_0^{t_1} dt_2\;\sum_k e^{iE_nt_1}\langle n|K|k\rangle\cos(\omega t_1)e^{-iE_kt_1}e^{iE_kt_2}\langle k|K|m\rangle\cos(\omega t_2)e^{-iE_mt_2} \\
&= A^2\int_0^t dt_1\int_0^{t_1} dt_2\;\sum_k K_{nk}K_{km}e^{i(E_n-E_k)t_1}\cos(\omega t_1)e^{i(E_k-E_m)t_2}\cos(\omega t_2) \\
&= \frac{A^2}{4}\int_0^t dt_1\int_0^{t_1} dt_2\;\sum_k K_{nk}K_{km}e^{i(E_n-E_k)t_1}\left(e^{i\omega t_1}+e^{-i\omega t_1}\right)e^{i(E_k-E_m)t_2}\left(e^{i\omega t_2}+e^{-i\omega t_2}\right)
\end{aligned}$$

Since the summation over k is an infinite sum, we cannot recklessly swap the order of integration and summation. Further tests will have to be carried out to determine whether swapping is permissible. Additionally, the K matrix is infinite-dimensional, so computing $\sum_k K_{nk}K_{km}$ in and of itself is impossible. This problem will also require further analysis to deal with. Due to the lack of such knowledge, we leave the result as it stands.

Annex B: MATLAB Code

The code was written in a MATLAB Live Script format due to its similarity to Jupyter Notebook. It was exported to the typical MATLAB format to be displayed here and will not run very well if run as a `.m` file.

```
%% QM3 Project
% Numerical simulation of the evolution of a wavepacket in a 1D harmonic trap
% using fast fourier transport (fft) method
%
% Unit of energy: hbar*omega, where h_bar is the Planck constant and omega is
% the frequency of the trap
%
% Unit of length: l=sqrt(h_bar/(m*omega)), where sqrt(...) is the square root
% function and m is the mass of the particle
%
% Unit of momentum: hbar/l
%
% energy unit: hbar\omega,  Hamiltonian --> dimensionless
%
% time dimensionless: omega*t    i d/dxt | >= dimension H |>
%
% dimensionless time = 2pi. one classical period

clc
clear
close all
%% Parameters of Simulation

a = -20;                          % Left end point
b = +20;                          % Right end point
L = b-a;                          % Width of the space
N = 512;                          % No. of cells
X = a+L*(0:N-1)/N;                % Dimensionless coordinates
P = (2*pi/L)*[0:N/2-1,-N/2:-1]; % Dimensionless momentum

T= 50*pi;                         % Duration of the evolution
M = 10^3;                         % Total number of steps in the evolution
dt = T/M;                         % Time step

X0 = 2.0;                         % Location of centre of wavepacket
sigma = 1.0;                      % Width of the initial wavepacket

A = 0.01;                         % Perturbation Amplitude
w = 0.99;                           % Perturbation Frequency
%% Defining the Hamiltionian
% We define 2 vectors that store the split-step propagators in position and
% momentum space respectively.
%
% Note that UV is only placed here for completeness. Since it depends on time,
% it must be defined in the loop over time later in the code.

%UV = exp(-1i*(X.^2/2 + A*sin(X)*cos(w*time))*dt/2);   % One-step propagator in position
    space, only taking diagonal form
UT = exp(-1i*(P.^2/2)*dt);                             % One-step propagator in momentum
    space
%% Defining & Initialising the HO Eigenstates

poly_0 = hermiteH(0,X);
ho_0_prep = poly_0.*exp(-(X(1:N)-X0).^2/(2*sigma^2));   % Ground state
ho_0=ho_0_prep/sqrt(sum(abs(ho_0_prep).^2));            % State normalisation

poly_1 = hermiteH(1,X);
ho_1_prep = poly_1.*exp(-(X(1:N)-X0).^2/(2*sigma^2));   % First excited state
ho_1=ho_1_prep/sqrt(sum(abs(ho_1_prep).^2));            % State normalisation

poly_2 = hermiteH(2,X);
ho_2_prep = poly_2.*exp(-(X(1:N)-X0).^2/(2*sigma^2));   % Second excited state
ho_2=ho_2_prep/sqrt(sum(abs(ho_2_prep).^2));            % State normalisation
```

```
62
63 poly_3 = hermiteH(3,X);
64 ho_3_prep = poly_3.*exp(-(X(1:N)-X0).^2/(2*sigma^2));   % Third excited state
65 ho_3=ho_3_prep/sqrt(sum(abs(ho_3_prep).^2));            % State normalisation
66
67 poly_4 = hermiteH(4,X);
68 ho_4_prep = poly_4.*exp(-(X(1:N)-X0).^2/(2*sigma^2));   % Fourth excited state
69 ho_4=ho_4_prep/sqrt(sum(abs(ho_4_prep).^2));            % State normalisation
70 %% Animation of the Probability Density of the Wavefunction in Unperturbed Hamiltonian
71
72 UV = exp(-1i*(X.^2/2)*dt/2);
73
74 figure;
75 wave = plot(X(1:N),abs(psi(1:N)).^2);   % plotting initial state
76 ylim([0 0.15])
77 hold on
78 plot (P(1:N),abs(psi(1:N)).^2)
79 psi_0=ho_2;
80
81 drawnow
82 for m = 1:M
83     psi_1 = UV.*psi_0;
84     phi_2 = fft(psi_1); %wavefunction in momentum space
85     phi_3 = UT.*phi_2;
86     psi_3 = ifft(phi_3);
87     psi_4 = UV.*psi_3;
88     psi_0 = psi_4;      %prepare a new cycle
89     set(wave, 'YData', abs(psi_0(1:N)).^2)
90     pause(0.05)
91 end
92 psi=psi_0;              %final state updated
93 %% Transition Probability (1)
94
95 psi_0 = ho_0;           % this is the state which evolves
96 phi_0 = ho_1;           % this is the state which we wish to compare psi_0 against
97
98 t = [0];
99 y = [0];
100 P = [0];
101
102 for m = 1:M
103
104     time = t(end) + dt;
105     num_prob = abs(dot(psi_0, phi_0))^2;
106     %theor_prob = (A^2/8)*exp(-1/2)*abs((exp(1i*(1-w)*time)-1)/(1-w))^2;       % hardcoded
        the transition probability derived from theory
107     theor_prob = (A^2/8)*exp(-1/2)*abs( (exp(1i*(1-w)*time)-1)/(1-w) + (exp(1i*(1+w)*time)
        -1)/(1+w) )^2;       % Non-RWA version
108
109     t(end+1) = time;
110     y(end+1) = num_prob;
111     P(end+1) = theor_prob;
112
113     UV = exp(-1i*(X.^2/2 + A*sin(X)*cos(w*time))*dt/2);
114
115     psi_1 = UV.*psi_0;
116     psi_2 = fft(psi_1);
117     psi_3 = UT.*psi_2;
118     psi_4 = ifft(psi_3);
119     psi_5 = UV.*psi_4;
120
121     psi_0 = psi_5;
122 end
123
124
125 str1 = sprintf('A = %.2f, w = %.2f (sim)', A, w);
126 plot(t, y, ...
127     'Color', '#E74C3C', ...
```

```
    'LineWidth', 2, ...
    'DisplayName', str1 ...
    );                % plot of simulated transition pobability
hold on

str2 = sprintf('A = %.2f, w = %.2f (theory)', A, w);
plot(t, P, ...
    'Color', '#9B59B6', ...
    'LineWidth', 2, ...
    'DisplayName', str2 ...
    );              % plot of theoretically derived transition probability
hold on


legend('FontSize',12);
xlabel('Time, T', 'FontSize', 14, 'FontWeight', 'bold');
ylabel('Probability, P', 'FontSize', 14, 'FontWeight', 'bold');

ax = gca;
ax.FontSize = 12;

grid on
%% Transition Probability (2)

psi_0 = ho_0;           % this is the state which evolves
phi_0 = ho_1;           % this is the state which we wish to compare psi_0 against

t = [0];
y = [0];
P = [0];

for m = 1:M

    time = t(end) + dt;
    num_prob = abs(dot(psi_0, phi_0))^2;
    %theor_prob = (A^2/8)*exp(-1/2)*abs((exp(1i*(1-w)*time)-1)/(1-w))^2;       % hardcoded
    the transition probability derived from theory
    theor_prob = (A^2/8)*exp(-1/2)*abs( (exp(1i*(1-w)*time)-1)/(1-w) + (exp(1i*(1+w)*time)
    -1)/(1+w) )^2;       % Non-RWA version

    t(end+1) = time;
    y(end+1) = num_prob;
    P(end+1) = theor_prob;

    UV = exp(-1i*(X.^2/2 + A*sin(X)*cos(w*time))*dt/2);

    psi_1 = UV.*psi_0;
    psi_2 = fft(psi_1);
    psi_3 = UT.*psi_2;
    psi_4 = ifft(psi_3);
    psi_5 = UV.*psi_4;

    psi_0 = psi_5;
end


str1 = sprintf('A = %.2f, w = %.2f (sim)', A, w);
plot(t, y, ...
    'Color', '#2980B9', ...
    'LineWidth', 2, ...
    'DisplayName', str1 ...
    );              % plot of simulated transition pobability
hold on

str2 = sprintf('A = %.2f, w = %.2f (theory)', A, w);
plot(t, P, ...
    'Color', '#1ABC9C', ...
    'LineWidth', 2, ...
```

```
    'DisplayName', str2 ...
    );              % plot of theoretically derived transition probability
hold on


legend('FontSize',12);
xlabel('Time, T', 'FontSize', 14, 'FontWeight', 'bold');
ylabel('Probability, P', 'FontSize', 14, 'FontWeight', 'bold');

ax = gca;
ax.FontSize = 12;

grid on

%ylim([0,0.1])
%% Transition Probability (3)

psi_0 = ho_0;           % this is the state which evolves
phi_0 = ho_1;           % this is the state which we wish to compare psi_0 against

t = [0];
y = [0];
P = [0];

for m = 1:M

    time = t(end) + dt;
    num_prob = abs(dot(psi_0, phi_0))^2;
    theor_prob = (A^2/8)*exp(-sigma/2)*sigma^(3)*abs((exp(1i*(1-w)*time)-1)/(1-w))^2;
    % hardcoded the transition probability derived from theory

    t(end+1) = time;
    y(end+1) = num_prob;
    P(end+1) = theor_prob;

    UV = exp(-1i*(X.^2/2 + A*sin(X)*cos(w*time))*dt/2);

    psi_1 = UV.*psi_0;
    psi_2 = fft(psi_1);
    psi_3 = UT.*psi_2;
    psi_4 = ifft(psi_3);
    psi_5 = UV.*psi_4;


    psi_0 = psi_5;
end


str1 = sprintf('A = %.2f, w = %.2f (sim)', A, w);
plot(t, y, ...
    'Color', '#F1C40F', ...
    'LineWidth', 2, ...
    'DisplayName', str1 ...
    );              % plot of simulated transition pobability
hold on

str2 = sprintf('A = %.2f, w = %.2f (theory)', A, w);
plot(t, P, ...
    'Color', '#27AE60', ...
    'LineWidth', 2, ...
    'DisplayName', str2 ...
    );              % plot of theoretically derived transition probability
hold on


legend('FontSize',12);
xlabel('Time, T', 'FontSize', 14, 'FontWeight', 'bold');
ylabel('Probability, P', 'FontSize', 14, 'FontWeight', 'bold');
```

```
261
262 ax = gca;
263 ax.FontSize = 12;
264
265 grid on
266 %% Fourier Transform of Probability
267
268 hold off
269
270 K = fft(P);
271
272 fs = 1/dt;
273 f = (0:length(K)-1)*fs/length(K);
274
275 plot(f,K, ...
276     'Color', '#27AE60', ...
277     'LineWidth', 2 ...
278     );
279
280 xlabel('Frequency, f', 'FontSize', 14, 'FontWeight', 'bold');
281 ylabel('Wave Amplitude, K', 'FontSize', 14, 'FontWeight', 'bold');
282
283 xlim([0,1])
284 ylim([-0.06,0.06])
285
286 grid on
```